Developmental Biology 341 (2010) 416–428

Contents lists available at ScienceDirect

Developmental Biology

journal homepage: www.elsevier.com/developmentalbiology

Genetic interaction between *Sox10* and *Zfhx1b* during enteric nervous system development

Laure Stanchina [a,b], Tom Van de Putte [c,d,1], Michel Goossens [a,b], Danny Huylebroeck [c,d], Nadege Bondurand [a,b,*]

[a] INSERM U955, IMRB, Equipe 11, Creteil, F-94010, France
[b] Universite Paris Est, Faculte de Medecine, Creteil, F-94010, France
[c] Laboratory of Molecular Biology (Celgen), Center of Human Genetics, University of Leuven, Belgium
[d] Department of Molecular and Developmental Genetics (VIB11), Flanders Institute of Biotechnology, B-3000 Leuven, Belgium

ARTICLE INFO

Article history:
Received for publication 24 November 2009
Revised 29 January 2010
Accepted 25 February 2010
Available online 4 March 2010

Keywords:
Differentiation
Enteric nervous system
Hirschsprung
Mowat–Wilson
Neural crest
Sox10
Transcription factor
Waardenburg
Zeb2
Zfhx1b

ABSTRACT

The involvement of *SOX10* and *ZFHX1B* in Waardenburg–Hirschsprung disease (hypopigmentation, deafness, and absence of enteric ganglia) and Mowat–Wilson syndrome (mental retardation, facial dysmorphy and variable congenital malformations including Hirschsprung disease) respectively, highlighted the importance of both transcription factors during enteric nervous system (ENS) development. The expression and function of SOX10 are now well established, but those of ZFHX1B remain elusive. Here we describe the expression profile of *Zfhx1b* and its genetic interactions with *Sox10* during mouse ENS development. Through phenotype analysis of *Sox10;Zfhx1b* double mutants, we show that a coordinated and balanced interaction between these two genes is required for normal ENS development. Double mutants present with more severe ENS defects due to decreased proliferation of enteric progenitors and increased neuronal differentiation from E11.5 onwards. Thus, joint activity between these two transcription factors is crucial for proper ENS development and our results contribute to the understanding of the molecular basis of ENS defects observed both in mutant mouse models and in patients carrying *SOX10* and *ZFHX1B* mutations.

Introduction

The enteric nervous system (ENS) is the part of the peripheral nervous system that controls the peristaltic and secretory activity of the gut wall (Gershon et al., 1994). It is composed of a large number of neurons and glial cells, which are organized into interconnected ganglia distributed throughout the length of the gut (Burns and Thapar, 2006; Furness, 2006; Hao and Young, 2009; Heanue and Pachnis, 2007). During embryogenesis, most of the ENS is derived from the vagal neural crest cells (Le Douarin and Kalcheim, 1999). A small portion also derives from the sacral region (Burns and Douarin, 1998). After delaminating from the neural tube, vagal neural crest cells enter the foregut at day E9.5 in mice and, migrating in a rostrocaudal direction, colonize the entire length of the gut by E15. Altered proliferation, survival, migration or differentiation of ENCC (Enteric Neural Crest Cells) result in an absence of enteric ganglia (aganglionosis), usually affecting the colon, and leading to severe constipation or intestinal obstruction (Hirschsprung disease, HSCR) (for review see (Amiel et al., 2008; Heanue and Pachnis, 2007). Studies performed so far led to the identification of critical players in ENS development, including the Receptor Tyrosine Kinase RET, its ligands GDNF and NTN, the G-coupled receptor EDNRB and its ligand endothelin-3, the BMP signaling pathway, KBP, β1 integrin and L1-CAM adhesion molecules, and the transcription factors PHOX2B, MASH1, HAND2, ZFHX1B and SOX10 (for review see (Amiel et al., 2008; Burns and Thapar, 2006; Burzynski et al., 2009; Hao and Young, 2009; Heanue and Pachnis, 2007).

SOX10 is a member of the high-mobility group-domain SOX family of transcription factors (for review, see (Bowles et al., 2000; Kelsh, 2006; Mollaaghababa and Pavan, 2003; Wegner, 1999; Wegner, 2005, 2009; Wilson and Koopman, 2002). In 1998, cloning and involvement of this gene in a spontaneous mouse model of Waardenburg–Hirschsprung disease (the Dom mouse presenting with hypopigmentation, deafness, and absence of enteric ganglia) showed its crucial role for proper neural crest cells development, and ENS and melanocytes in particular (Herbarth et al., 1998; Southard-Smith et al., 1998). Invalidation of this gene by targeted gene deletion confirmed these observations (Britsch et al., 2001). Indeed, at the heterozygous state, both mouse mutants exhibit pigmentation defects

* Corresponding author. INSERM U955, Equipe 11, Hôpital Henri Mondor, 51 Avenue du Maréchal de Lattre de Tassigny, 94010, Créteil, France. Fax: +33 148993345.
E-mail address: nadege.bondurand@inserm.fr (N. Bondurand).
[1] Present address: Tigenix S.A., Romeinse straat 12 box 2, B-3001 Leuven, Belgium.

0012-1606/$ – see front matter © 2010 Elsevier Inc. All rights reserved.
doi:10.1016/j.ydbio.2010.02.036

and absence of enteric ganglia from a variable length of the colon. Homozygous mutant mice on the other hand have severe deficits in several neural crest derivatives, including complete lack of ENS (Britsch et al., 2001; Herbarth et al., 1998; Kapur, 1999; Southard-Smith et al., 1998).

During mouse development, *Sox10* is first expressed in neural crest cells, including cells of vagal origin, as they delaminate from the neural tube. At this stage, SOX10 protein appears to be required for the survival and the maintenance of these cells prior to lineage segregation (Honore et al., 2003; Kapur, 1999; Kim et al., 2003). When they enter the foregut, all ENCC express *Sox10*, which is considered a marker of ENS progenitors (for review, see (Heanue and Pachnis, 2007)). In partial absence of *Sox10*, mice possess a smaller pool of ENS progenitors, strongly suggesting a role for this HMG-type transcription factor in maintaining progenitor state (Paratore et al., 2002). Later, *Sox10* is expressed in glial cells but switched off in neurons (Bondurand et al., 2003; Young et al., 2003), and it is proposed to function in cell fate specification and glial cell differentiation (for review, see (Heanue and Pachnis, 2007)). Extinction of this gene seems to be a prerequisite for complete neuronal differentiation. Consistent with these observations, constitutive expression of *Sox10* inhibits overt neuronal differentiation in cultured ENCC (Bondurand et al., 2006).

An increasing number of molecular and developmental studies revealed that interactions between SOX10 and other pathways are crucial for proper ENS development. Genome-wide association studies performed in mice as well as phenotypic analysis of mouse double mutants revealed interactions between *Sox10* and loci located on chromosomes 3, 5, 8, 11 and 14 as well as with *Sox8*, *Ret*, and *endothelin-3*/*Ednrb* (Cantrell et al., 2004; Lang et al., 2000; Maka et al., 2005; Owens et al., 2005; Stanchina et al., 2006; Zhu et al., 2004). It now seems crucial to expand this gene network and identify which other factors could interact with *Sox10*, thus controlling multi-lineage ENS progenitor maintenance and enteric differentiation.

ZFHX1B (Zinc Finger HomeoboX 1b; also known as ZEB2, Zinc finger E-box Binding homeobox 2 or SIP1, Smad Interacting Protein 1) belongs to the Zfhx1 family proteins in vertebrates. Originally described as transcriptional repressors, these transcription factors are characterized by a homeodomain-like domain and two separated clusters of multiple zinc fingers (Postigo and Dean, 2000; van Grunsven et al., 2001; Verschueren et al., 1999). ZFHX1B was identified in a yeast two-hybrid screen as a protein binding to the MH2 domain of Smad1 (Verschueren et al., 1999) and is therefore a candidate component of the signal transduction pathways triggered by the Smad effector proteins of the TGF-β/BMP family (Eisaki et al., 2000; Postigo, 2003; van Grunsven et al., 2001). Numerous studies have shown that it is involved in neural specification where it has been proposed to transcriptionally inhibit BMP production (Eisaki et al., 2000; Nitta et al., 2007, 2004; Van de Putte et al., 2003; van Grunsven et al., 2007). Recent studies in *Xenopus* have shown that XSIP1 binds directly to the proximal promoter of *Bmp4* and represses expression of this gene (van Grunsven et al., 2007). ZFHX1B has also been shown to play an important role in epithelial–mesenchymal transition (EMT) by repressing several adhesion molecules including E-cadherin (Comijn et al., 2001; van Grunsven et al., 2003; Vandewalle et al., 2005).

The role of ZFHX1B in ENS development was first highlighted by its involvement in Mowat–Wilson syndrome, a dysmorphic and severe mental retardation syndrome with occurrence of Hirschsprung disease or constipation (Cacheux et al., 2001; Dastot-Le Moal et al., 2007; Garavelli et al., 2009; Wakamatsu et al., 2001; Zweier et al., 2005). Generation of *Sip1*/*Zfhx1b*/*Zeb2* knock-out mice revealed that it is essential for specification of sufficient numbers of vagal neural crest cells (Higashi et al., 2002; Van de Putte et al., 2003). Heterozygous animals present with no apparent gross morphological defects except an absence of corpus callosum, but homozygotes die at E9.5 and present with cardiovascular dysfunction, an aberrant neural plate, failure of the neural tube to close, and shortened somites. More importantly, *Zfhx1b* homozygous embryos show a delay in cranial neural crest migration and the near-absence of vagal neural crest formation (Van de Putte et al., 2003). Recently, a conditional knock-out has been generated in which *Zfhx1b* was specifically removed in neural crest cells using a Wnt1-Cre crossing strategy. Homozygous mice present with specific abnormalities in craniofacial, heart, melanocytes and peripheral nervous system development as well as severe intestinal aganglionosis (Van de Putte et al., 2007). In human, mice and zebrafish, preliminary expression studies revealed the presence of *Zfhx1b* within vagal enteric precursor cells upon gut invasion. Later during development, the whole ENS is heavily expressing this factor (Bassez et al., 2004; Delalande et al., 2008; Espinosa-Parrilla et al., 2002; Van de Putte et al., 2007). However, the spatio-temporal expression profile and function of ZFHX1B during ENS development and differentiation as well as its interaction with other ENS factors remain poorly studied.

Here we analyzed the expression of *Zfhx1b* and explored the possibility of genetic interactions between this gene and *Sox10* during ENS development. To this end, we crossed the conventional *Zfhx1b* mutant with the *Sox10* knock-out mouse, compared the enteric phenotype of single and double heterozygous animals, and investigated the cellular origin of the observed ENS defects.

Materials and methods

Animals, pups, embryos collection and genotyping

The generation of $Sox10^{LacZ}$ and $Zfhx1b^{\Delta ex7}$ animals have been described previously (Britsch et al., 2001; Higashi et al., 2002; Van de Putte et al., 2003). $Sox10^{LacZ}$ mice were backcrossed on C3HeB/FeJ for at least 4 generations before use. $Zfhx1b^{\Delta ex7}$ were generated and maintained on CD1 background. Alternatively, $Zfhx1b^{\Delta ex7}$ were crossed on C3HeB/FeJ background. Similar results were obtained whatever the genetic background used. The genotype of mice and embryos was determined by PCR analysis of genomic DNA extracted from a tail tip fragment or yolk sac, respectively using PCR primers previously described (Britsch et al., 2001; Van de Putte et al., 2007), except for Zfhx1b-intron6R which was modified as follows: 5′-ATCAGCAGCCTCCTATTTAAACAGAGTGTC-3′. $Zfhx1b^{\Delta/+}$ mice were crossed with $Sox10^{LacZ/+}$ to generate embryos and pups. Embryos from E9.5 to E15.5 were obtained from staged pregnancies. The day of vaginal plug was considered to be E0.5.

Dissected guts or embryos were fixed one to two hours in 4% paraformaldehyde at 4 °C. After fixation, 8 μm frozen sections of embryos of different genotypes were generated. Dissected guts or sections were used for immunohistochemistry. Alternatively, whole embryos or dissected guts were fixed in 1% paraformaldehyde and 0.2% glutaraldehyde and used for whole-mount X-Gal staining.

Acute cultures

Acute cultures of guts were performed as described (Barlow et al., 2003). Briefly, guts were dissected from E11.5 or E13.5 embryos of different genotypes, stomach region was removed and intestine was incubated with dispase/collagenase (0.5 mg/ml in PBS1X, Roche) for 5 min at room temperature. Digested tissues were washed twice with 1× PBS, dissociated by repeated pipetting, and plated on fibronectin coated (20 μg/ml) SONIC-SEAL wells (VWR) in optiMEM (Life technologies). After a few hours in an atmosphere of 5% CO_2, most cells were adherent and no differential cell adherence was observed between the genotypes as assessed by counting the number of cells before and after plating (DAPI staining). Cultures were fixed 10 min in 4% paraformaldehyde at 4 °C, and used for immunohistochemistry.

Immunostaining and X-Gal staining

Immunostaining was performed as previously described (Barlow et al., 2003; Bondurand et al., 2003). The following primary antibodies were used in various combinations: TuJ1 (mouse, 1:1000 dilution, Eurogentec), phospho-histone 3 (PH3, rabbit, 1:500 dilution, Upstate), activated-Caspase-3 (casp3, rabbit, 1:200 dilution, Cell Signaling), Sox10 (rabbit, 1:200 dilution, Chemicon), Sox10 (guinea pig, 1:500 dilution, kindly provided by Dr. M. Wegner; (Maka et al., 2005)), Phox2b (rabbit, 1:500 dilution, kindly provided by Dr. J.F. Brunet; (Pattyn et al., 1997)), B-FABP (rabbit, 1:5000 dilution, kindly provided by Dr. T. Müller; (Kurtz et al., 1994)), GFAP (Rabbit, 1:400 dilution, Dakocytomation), and Zfhx1b (rabbit; 1:50; kindly provided by D. Huylebroeck; (Seuntjens et al., 2009)). Secondary antibodies used were as follows: anti-mouse FITC conjugated (1:150 dilution, Sigma), anti-mouse alexaFluor568 (1:500 dilution, Invitrogen), anti-rabbit FITC conjugated (1:150 dilution, Sigma), anti-rabbit Cy3 (1:150 dilution, Sigma), and anti-guinea pig Cy3 (1:200 dilution, Dianova). Preparations were mounted directly in Vectashield containing DAPI (Vector laboratories). X-Gal staining followed standard procedures. Sections, guts or cultures were examined with a Leica DMR microscope equipped with a Hamamatsu digital camera or Olympus SZH10 and Leica MZ6 stereo microscope coupled to Visilog capture program.

Results

Zfhx1b expression in progenitor and glial cells during ENS development

To gain insight into ZFHX1B function during ENS development, we first compared its expression pattern to that of SOX10. To this end, we performed co-immunohistochemistry with antibodies against Zfhx1b and Sox10, TuJ1 or GFAP on wild-type embryos sections from E9.5 to birth. We observed that ZFHX1B was present in all SOX10-positive vagal crest cells from E9.5 onwards. Indeed, at E9.5/E10, double labeled Sox10/Zfhx1b cells were found closely apposed to the lateral and ventral part of the dorsal aorta as well as entering the foregut (Fig. 1 A and inserts A1 to A3). Later during development, ZFHX1B protein is found in almost all SOX10-positive cells within enteric ganglia (Fig. 1 B, D and inserts B1–3 and D1–3). Upon differentiation, ZFHX1B protein is downregulated in neuronal cells. Indeed, it is absent from cells expressing the neuron specific class III β-tubulin (identified by TuJ1 antibody; Fig. 1 C, E and inserts C1–3 and E1–3). In contrast, it is present in ENCC acquiring a glial cell fate (GFAP-expressing cells, Fig. 1 F and G and inserts F1–3, G1–3). Altogether these results suggest that ZFHX1B, similar to SOX10, is present in enteric progenitors and glia as ENS development proceeds, but is switched off in neurons. Interestingly, sections across the stomach region performed at E13.5 revealed that ZFHX1B is not restricted to ENCC and glial derivatives. It is also found in mesenchymal cells adjacent to the epithelium, in a region previously described as containing BMP4-expressing cells (Fu et al., 2006).

Genetic interactions between Sox10 and Zfhx1b during ENS development

The overlap between SOX10 and ZFHX1B expression profiles led us to speculate that both factors could control various steps of ENCC in an additive or cooperative manner. To test the possibility of a genetic interaction between both loci, we exploited the availability of mice with targeted mutation within each of these genes (for details regarding mouse models, see Materials and methods). We crossed *Sox10* and *Zfhx1b* heterozygous mice and compared the enteric phenotype of single and double heterozygous mice. As distribution of enteric neurons along the gut reflects the progress of migration and differentiation of ENCC, we first compared neurogenesis in the gut of embryos of different genotypes using whole-mount immunostaining with TuJ1, an appropriate marker to visualize complete colonization of the gut in wild-type mouse embryos at E13.5 (Barlow et al., 2003; Stanchina et al., 2006).

Consistent with previous findings, we observed no significant difference in the intensity or distribution of staining between wild-type and *Zfhx1b* heterozygous guts (Fig. 2, compare panels A1–5 with B1–5). In contrast, we observed a migration delay in the majority of $Sox10^{LacZ/+}$ single mutants (Fig. 2 C1–5). TuJ1-positive cells were missing from the caecum onwards in 2/3rd of the guts analyzed (Fig. 2 E). More importantly, all guts from $Sox10^{LacZ/+}$;$Zfhx1b^{\Delta/+}$ showed a severe colonization delay compared to single mutants. Indeed, TuJ1 staining stopped within the first half of the small intestine in 4 out of 7 guts, or before the caecum entry in 3 out of 7 guts (Fig. 2 D1–5 and E). Interestingly, complete disorganization of the neuronal network was also clearly visible in colonized regions of all double heterozygous guts (e.g., see the reduction in the number of neurons and the enhanced ganglion cell aggregation observed in Fig. 2 G; compare to F). Thus, removal of one *Zfhx1b* allele in *Sox10* heterozygous animals results in an ENS phenotype that is much more severe than that of single mutants, confirming a strong genetic interaction between these two genes during ENS development.

To determine whether the observed defects reflect the absence of enteric progenitor cells expressing *Sox10* or defects in neuronal differentiation, we took advantage of the LacZ reporter present in the $Sox10^{LacZ}$ allele and performed staining with X-Gal on whole-mount gut preparations. When staining of $Sox10^{LacZ/+}$;$Zfhx1b^{\Delta/+}$ guts was compared to that of $Sox10^{LacZ/+}$, a strong colonization delay was observed in all cases (compare Fig. 3 A with B). Indeed, staining stopped halfway through the small intestine of the 6 double heterozygous embryos that were analyzed. In contrast, $Sox10^{LacZ/+}$ littermates presented with no defects or with an absence of staining, which is limited to the second half of the caecum and/or the colon. The enteric defects observed in $Sox10^{LacZ/+}$;$Zfhx1b^{\Delta/+}$ therefore result from the absence of enteric progenitor cells along a variable length of the intestine. A complete disorganization of the enteric network was also clearly visible within colonized regions of double mutants (compare A1 and B1), similar to the respective patterns observed via staining for TuJ1.

Absence of ENS defects in E9.5/E10 embryos with Sox10 and Zfhx1b deficiencies

To determine the origin of the ENS defects, we extended our analyses to earlier time points, and first compared the behavior of vagal neural crest cells around the time of foregut invasion (from E9.5 to E10.5). X-Gal staining performed on whole-mount embryos revealed no apparent defects in double heterozygous embryos as compared to $Sox10^{LacZ/+}$ littermates (Fig. 4 A and data not shown). Indeed, ENCC were found to migrate within the foregut of all E9.5 and E10.5 embryos analyzed, in a very similar pattern (compare Fig. 4 A6 to A5, and data not shown). For example, at E10.5, and irrespective of the genotypes of the respective embryos, cells were visualized within the stomach region and migrated in chain to colonize the small

Fig. 1. Zfhx1b profile during ENS development. (A) Zfhx1b (Green)/Sox10 (Red) double immunostaining of sections of E9.5/E10 wild-type embryos. Inserts A1–3 represent higher magnifications of the boxed region in A and show that Zfhx1b and Sox10 co-localize in most vagal neural crest cells upon gut colonization. The white dotted lines indicate the foregut region. (B, C) Immunostaining on sections through the stomach of E10.5/E11.5 and (D, E, F) E13.5 embryos using anti-Zfhx1b, Sox10, TuJ1 and GFAP antibodies revealed a strong Zfhx1b staining in the nuclei of Sox10 undifferentiated ENCC (B and D), presence of Zfhx1b in GFAP + glial cells (F), and a downregulation of Zfhx1b in TuJ1+ neuronal cells (C, E). (G) Immunostaining on sections through the intestine of adult mice using anti-Zfhx1b and GFAP antibodies confirm Zfhx1b presence in glial cells. Dotted lines in B, C, D, E, F, G indicate the stomach lumen. Inserts B1–3, C1–3, D1–3, E1–3, F1–3, G1–3 represent higher magnifications of B to G, respectively. Note also the presence of Zfhx1b in mesenchymal cells adjacent to the stomach epithelium at E13.5 (D–F).

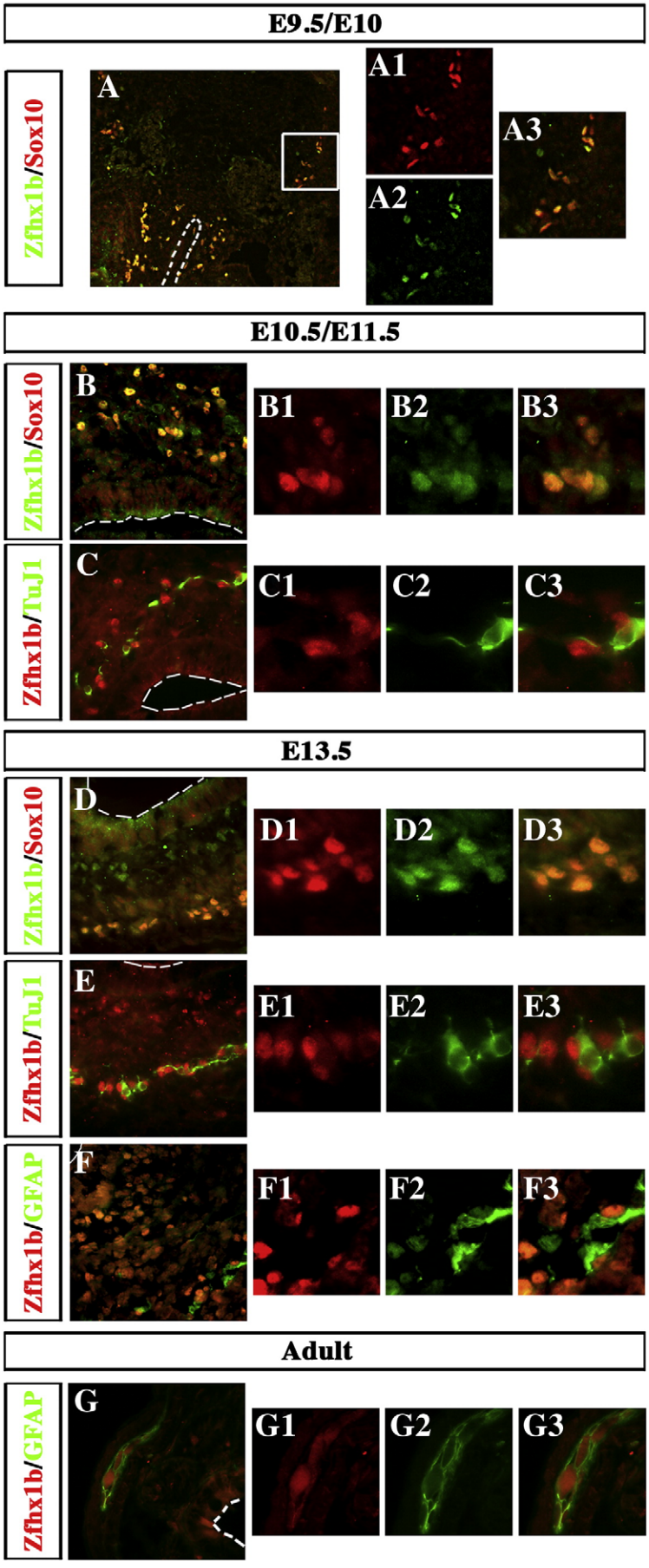
E9.5/E10
Zfhx1b/Sox10
A
A1
A2
A3
E10.5/E11.5
Zfhx1b/Sox10
B
B1
B2
B3
Zfhx1b/TuJ1
C
C1
C2
C3
E13.5
Zfhx1b/Sox10
D
D1
D2
D3
Zfhx1b/TuJ1
E
E1
E2
E3
Zfhx1b/GFAP
F
F1
F2
F3
Adult
Zfhx1b/GFAP
G
G1
G2
G3

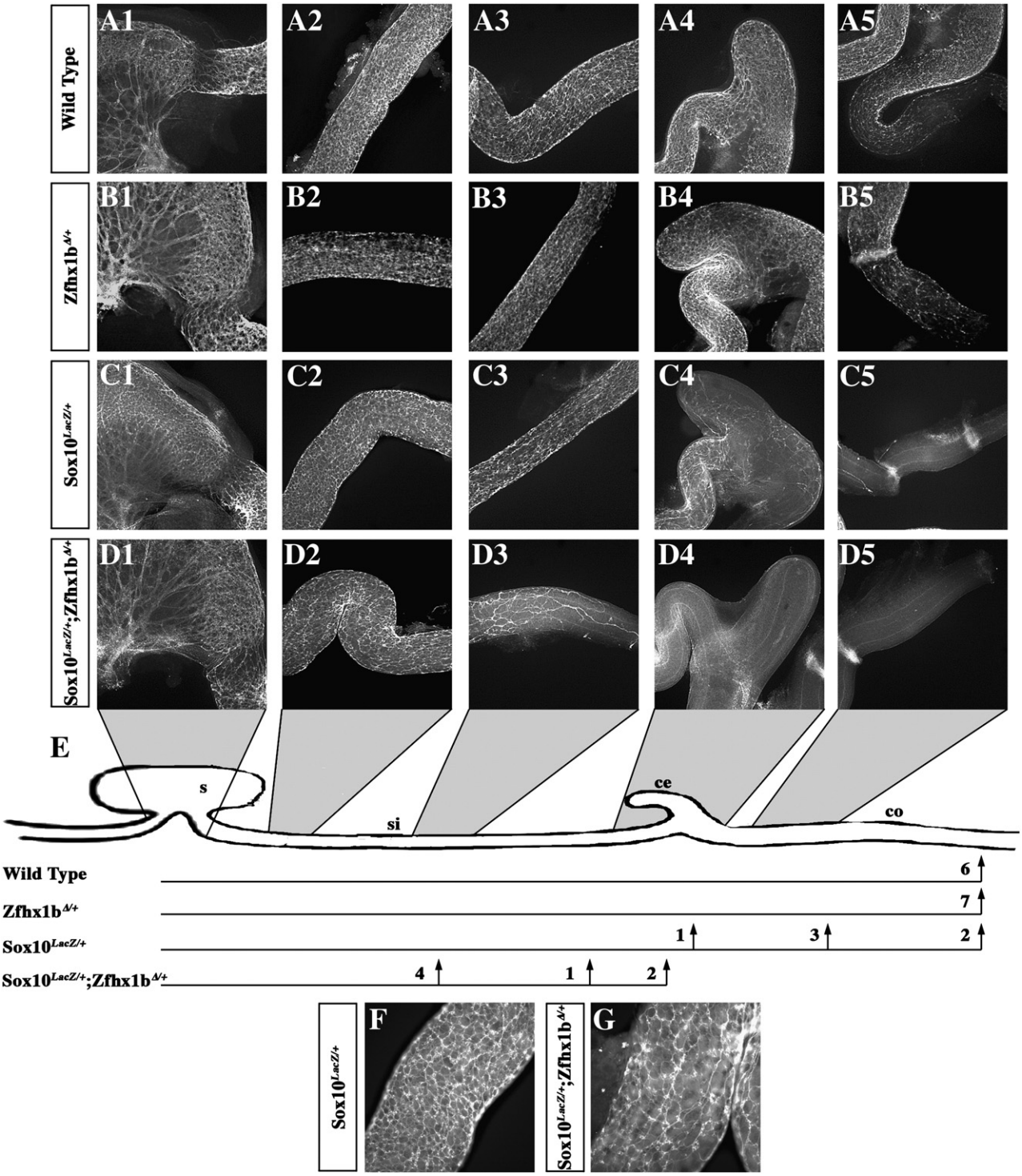

Fig. 2. Genetic interaction between Sox10 and Zfhx1b controls ENS development. Whole-mount TuJ1 immunohistochemistry was performed on E13.5 guts from wild-type (A1–5), Zfhx1b$^{\Delta/+}$ (B1–5), Sox10$^{LacZ/+}$ (C1–5) and Sox10$^{LacZ/+}$;Zfhx1b$^{\Delta/+}$ (D1–5) embryos. Panels A1 to D1, A2 to D2, A3 to D3, A4 to D4, A5 to D5 show staining in the distal stomach, the first part and middle of the small intestine, the caecum and the colon, respectively. (E) Schematic representation of the gut. The shaded areas on top of this scheme represent the regions of the gut shown in A to D. Below this scheme, the lines and perpendicular arrows indicate the extent of colonization for each class of genotyped embryos. The number of embryos presenting with a defined defect are indicated on the left of each arrow. Note the severe delay in colonization in double heterozygous animals (D1–5 and E) compared to the respective single mutants (B1–5 and C1–5 and E). F and G represent higher magnifications of C2 and D2 respectively. Note the disorganized network of neurons observed in G. s: stomach; si: small intestine; ce: caecum; co: colon.

intestine (Fig. 4 A). Interestingly, X-Gal staining performed on E10.5 embryos revealed no apparent defects in other neural crest derivatives either. Indeed, general observation of cranial ganglia, dorsal root ganglia and peripheral nerves revealed no differences between Sox10$^{LacZ/+}$ and Sox10$^{LacZ/+}$;Zfhx1b$^{\Delta/+}$ embryos (compare Fig. 4 A2 to A1 and A4 to A3).

To complete these observations, we labeled sections of E9.5 embryos of different genotypes with anti-Sox10 antibody to compare the number of vagal neural crest cells invading the foregut region and with activated-Caspase-3 to document apoptosis within and outside of the gut (Fig. 4 B). In sections of wild-type embryos, as well as of Zfhx1b$^{\Delta/+}$, an apparent equal number of cells were observed that

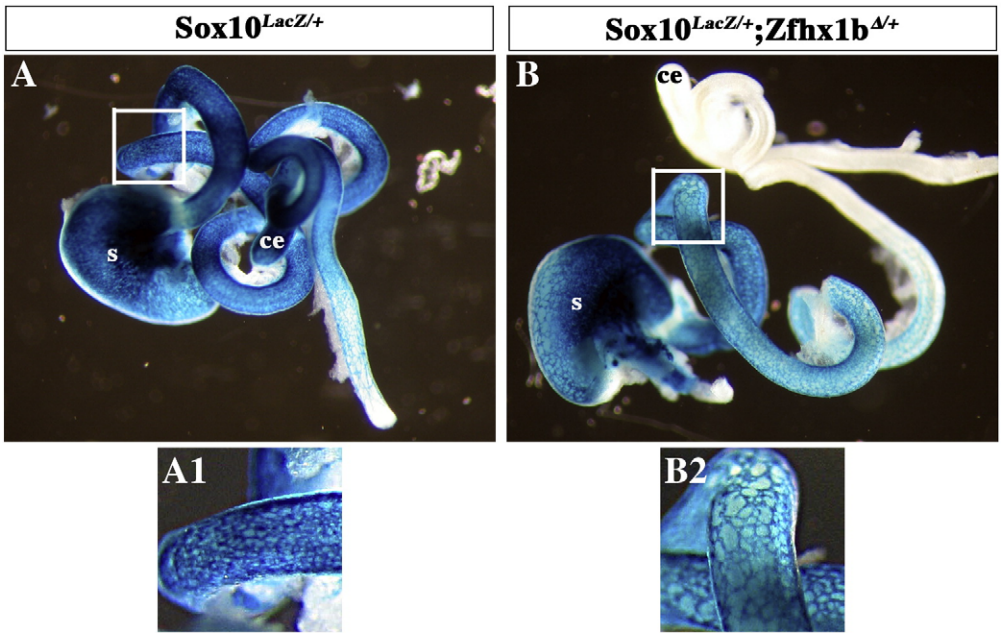

Fig. 3. ENS phenotype in double heterozygous mice results from an absence of enteric progenitor cells. Whole-mount X-Gal staining was performed on E13.5–14 guts from $Sox10^{LacZ/+}$ (A) and $Sox10^{LacZ/+}$;$Zfhx1b^{\Delta/+}$ (B) embryos. Note the absence of X-Gal staining halfway through the small intestine of $Sox10^{LacZ/+}$;$Zfhx1b^{\Delta/+}$ embryos. s: stomach. Ce: caecum. A1 and B1 represent higher magnifications of boxed regions in A and B. Note the reduced number of cells and disorganized network in $Sox10^{LacZ/+}$;$Zfhx1b^{\Delta/+}$ embryos.

migrated in the foregut and only few Caspase-3 positive cells were detected (Fig. 4 B1 to B4). As previously described, we observed few apoptotic cells in the stream of migrating ENCC in $Sox10^{LacZ/+}$ (Fig. 4 B5–6 and (Maka et al., 2005; Stanchina et al., 2006). We made similar observations when $Sox10^{LacZ/+}$;$Zfhx1b^{\Delta/+}$ mutants were analyzed, but the number of Sox10-positive migrating cells was comparable to that observed in wild-type embryos (Fig. 4 B7–8 and data not shown). Taken together, these results clearly show that ENCC migration in double heterozygous mouse embryos is not altered up to E10.5. The ENS defects observed in such mutant mice are thus neither due to increased cell death nor abnormal migration of vagal neural crest cells prior or at the time of foregut invasion.

Sox10;Zfhx1b double heterozygous embryos show severe but restricted ENS defects at E11.5

We then extended our analysis beyond these time points and analyzed the enteric phenotype of embryos of different genotypes only one day later. X-Gal staining performed on whole-mount embryos as well as TuJ1 staining performed on E11.5 whole-mount gut preparations revealed an apparent normal pattern of ENCC migration or a slight delay in $Zfhx1b^{\Delta/+}$ or $Sox10^{LacZ/+}$ embryos compared to wild-type embryos. Indeed, the vast majority of single heterozygous mice presented with cells in the stomach, the small intestine, and the wavefront of migrating ENCC was seen entering the caecum area (See Fig. 5 A3 and data not shown). In contrast, we observed a dramatic reduction in the number of X-Gal and TuJ1-positive cells in the gut of $Sox10^{LacZ/+}$;$Zfhx1b^{\Delta/+}$embryos. Indeed, the wavefront of migrating ENCC seemed severely delayed in all double heterozygous embryos analyzed ($n=6$, compare Fig. 5 A4 to A3 and data not shown; note that 2 out of 6 embryos presented with X-Gal-positive cells up to 3/4th of the small intestine, whereas 4 out of the 6 embryos presented with positive cells up to 1/3rd or halfway through the small intestine only). In agreement with observations made at E13.5, a complete disorganization of the network was also clearly visible in colonized regions of all E11.5 double heterozygous embryos (see the reduction in the number of X-Gal-positive cells in the inserts of panels A4; compare to A3). Thus, a severe ENS phenotype is seen from E11.5 onwards. At that stage, cells seem to be able to reach the stomach but fail to colonize the vast majority of the small intestine and more distal parts of the gastrointestinal tract.

Similar to E10.5 results, X-Gal staining revealed no apparent defects of other neural crest derivatives at E11.5. Indeed, general observation revealed no abnormal formation of cranial ganglia, dorsal root ganglia (DRG) or peripheral nerves in $Sox10^{LacZ/+}$;$Zfhx1b^{\Delta/+}$ embryos compared to $Sox10^{LacZ/+}$ littermates (compare Fig. 5 A2 to A1). The presence and the function of ZFHX1B and SOX10 in melanocytes and glial cells of the peripheral nervous system (Britsch et al., 2001; Van de Putte et al., 2007; Wegner, 2005) also prompted us to examine the formation of these derivatives in E11.5 $Sox10^{LacZ/+}$;$Zfhx1b^{\Delta/+}$ embryos. Taking advantage of the LacZ reporter within the $Sox10^{LacZ}$ allele, we first observed migration of melanoblasts. Irrespective of the genotypes, migrating melanoblasts were seen in the head (compare Fig. 5 B2 to B1), the cranial region (compare B4 to B3) and reaching the base of the hindlimb (compare B6 to B5), suggesting no apparent defects in double heterozygous embryos. In parallel, sections of E11.5 wild-types, single and double heterozygous embryos were labeled with anti-TuJ1 and anti-B-FABP (brain-specific fatty acid binding protein) antibodies in order to visualize neurons and glial cells, respectively, in DRG and along spinal nerves. B-FABP-positive cells were abundant in both areas in all embryos, suggesting normal glial cell differentiation in double mutants and single mutants (compare Fig. 5 C4 to C1–3). The phenotype of embryos with combined *Sox10;Zfhx1b* mutations thus suggests a specific cooperative requirement of both factors during ENS development only.

Cellular mechanism at the origin of the ENS defects observed in E11.5 and E13.5 embryos with Sox10 and Zfhx1b deficiencies

To determine the cellular defects underlying the ENS phenotypes observed in E11.5 and E13.5 $Sox10^{LacZ/+}$;$Zfhx1b^{\Delta/+}$ embryos, we quantified the pool of enteric progenitor cells and analyzed their proliferation and differentiation capacities.

We first quantified the number of progenitor cells on cultures of acutely dissociated guts at E11.5 by counting Phox2b-positive cells (which identifies ENCC progenitors and derivatives (Young et al., 2003)) and the fraction of these that were co-labeled with Sox10 (which identifies progenitor cells at that stage). In agreement with the

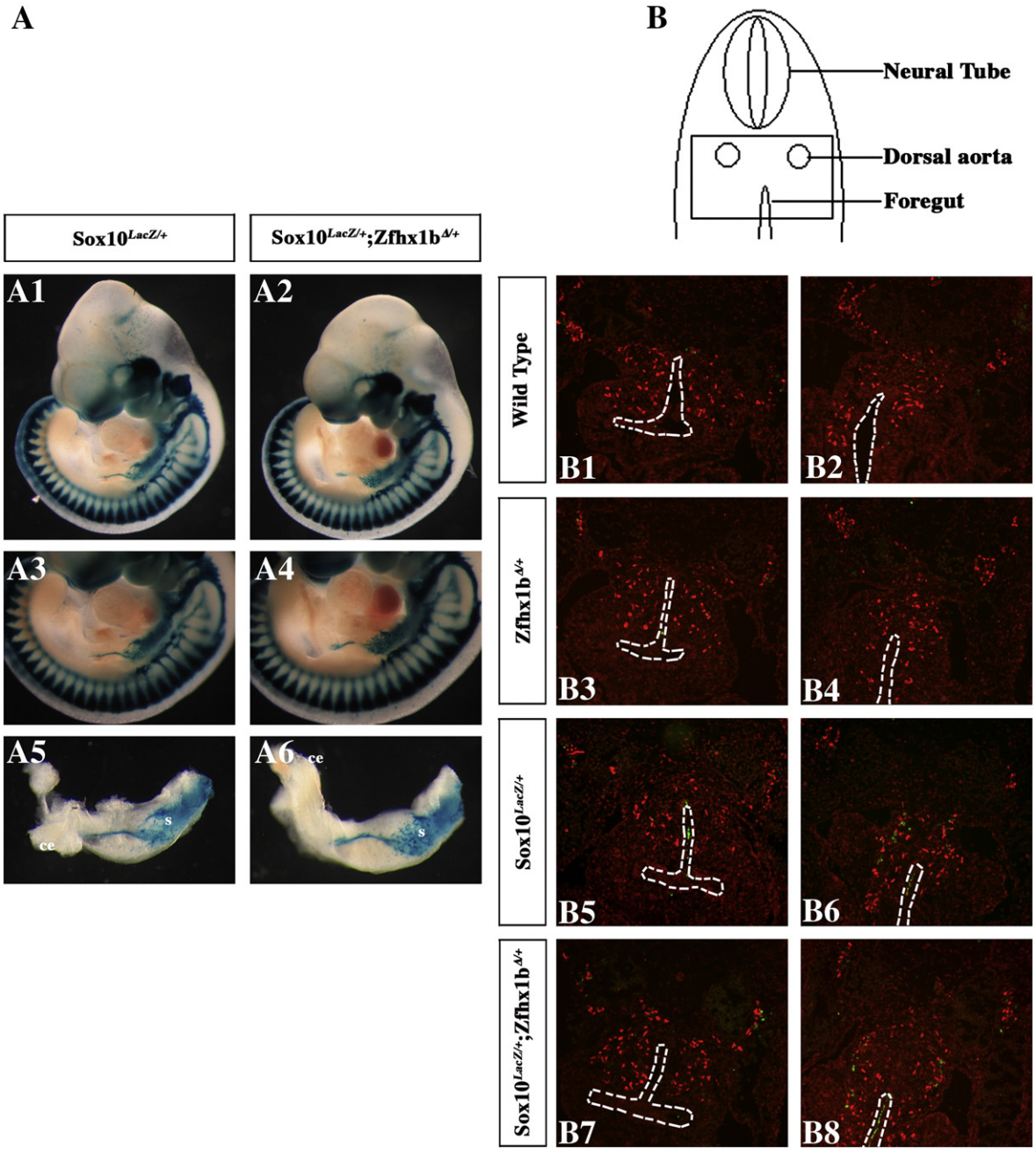

Fig. 4. Absence of ENS defects in Sox10;Zfhx1b double heterozygous mutant embryos at E10–E10.5. (A) Whole-mount X-Gal staining of E10.5 $Sox10^{LacZ/+}$ and $Sox10^{LacZ/+}$;$Zfhx1b^{\Delta/+}$ embryos. A3 and A4 represent higher magnifications of A1 and A2, respectively. A5 and A6 panels have been obtained after dissection of the gut, allowing better visualization of ENCC migration along the foregut. Note the absence of defects in $Sox10^{LacZ/+}$;$Zfhx1b^{\Delta/+}$ at this stage. s: stomach. ce: caecum (B) Scheme of the area shown in B1 to B8. (B1–8) Immunohistochemistry on sections of E10 wild-type (B1–2), $Zfhx1b^{\Delta/+}$ (B3–4), $Sox10^{LacZ/+}$ (B5–6), and $Sox10^{LacZ/+}$;$Zfhx1b^{\Delta/+}$ (B7–8) embryos, using anti-Sox10 (Red) and anti-Caspase-3 (Green) antibodies. White dotted lines indicate the esophagus tracheal (B1, 3, 5, 7) and foregut (B2, 4, 6, 8) regions. Note the absence of apoptosis and normal number of vagal crest cells in $Sox10^{LacZ/+}$;$Zfhx1b^{\Delta/+}$ at this stage.

X-Gal staining experiments (see Fig. 5), we observed a significant decrease in the number of Sox10-positive cells in $Sox10^{LacZ/+}$;$Zfhx1b^{\Delta/+}$ embryos compared to controls (Fig. 6 A). Indeed, the percentage of Sox10-positive cells among the Phox2b population in wild-type, $Zfhx1b^{\Delta/+}$, $Sox10^{LacZ/+}$ or $Sox10^{LacZ/+}$;$Zfhx1b^{\Delta/+}$ cultures were $23 \pm 7\%$, $15 \pm 4\%$, $14 \pm 6\%$ and $6 \pm 3\%$ respectively (with p values ranging from 0.0058 to 0.038 when $Sox10^{LacZ/+}$;$Zfhx1b^{\Delta/+}$ cultures were compared to wild-types or $Sox10^{LacZ/+}$ littermates). This reduction of enteric progenitor cells is therefore likely to contribute to the more severe ENS phenotype observed in the double heterozygous mutants.

We next attempted to quantify the proliferation capacities of these enteric progenitor cells by counting the fraction of Sox10-positive cells that co-labeled with the proliferation marker phospho-histone3. A significant decrease in proliferation was observed in double heterozygous mutants compared to controls (Fig. 6 B), thus demonstrating that the observed reduction in the pool of Sox10-positive cells is at least partially due to a reduction in the proliferation capacities of these cells.

Finally, we examined the possibility that the absence of ENCC halfway through the small intestine of double heterozygous mutants as well as the disorganized network observed in colonized regions could result from increased differentiation. We first analyzed the overall neuronal differentiation in E11.5 and E13.5 embryos of different genotypes (see Fig. 6 C and D, respectively). To this end, we determined the fraction of Phox2b population that co-labeled with

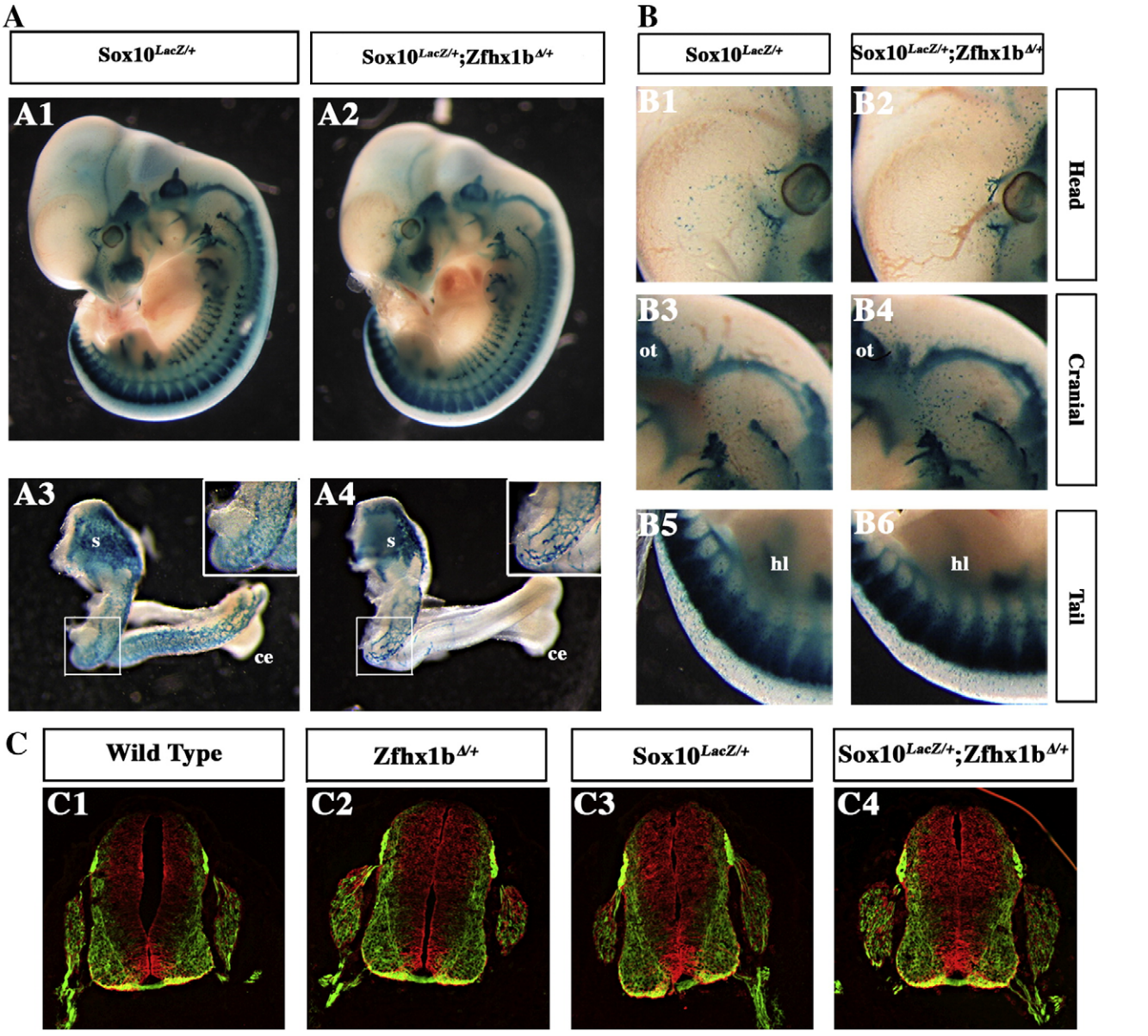

Fig. 5. Phenotype of E11.5 Sox10;Zfhx1b double heterozygous embryos. (A) Whole-mount X-Gal staining of mouse embryonic guts of the indicated genotype. A3 and A4 panels have been obtained after dissection of the guts, allowing better visualization of ENCC. The inserts in panels A3 and A4 represent higher magnification of boxed regions. Note the severe ENS migration delay in $Sox10^{LacZ/+}$;$Zfhx1b^{\Delta/+}$ (compare A3 to A4), the reduced number of cells, and the disorganized network in $Sox10^{LacZ/+}$;$Zfhx1b^{\Delta/+}$ embryos (compare insets in A3 and A4). s: stomach; ce: caecum (B) Melanoblasts in E11.5 $Sox10^{LacZ/+}$ and $Sox10^{LacZ/+}$;$Zfhx1b^{\Delta/+}$ embryos. X-Gal staining was used to visualize presence of melanoblasts in the head (B1–2), cranial (B3–4) and tail (B5–6) regions, respectively. Note the presence of migrating melanoblasts in $Sox10^{LacZ/+}$;$Zfhx1b^{\Delta/+}$ embryos. e: eye; ot: otic vesicle; hl: hindlimb. (C) Immunohistochemistry in transversal sections (neural tube and DRG region) of E11.5 embryos of indicated genotype using anti-TuJ1 (Red) and anti-B-FABP (Green) antibodies. Note the absence of gross DRG anomalies (compare A1 to A2; and C4 to C1–3).

the neuronal marker TuJ1, and found no significant difference in the percentage of double-positive (Phox2b + TuJ1 +) cells between wild-type and single mutant embryos. However, a slight but significant increase in overall neuronal differentiation was observed in double heterozygous mutants. Indeed, an increase of about 15% was observed in these mutant embryos compared to controls at both stages (with p values ranging from 0.0054 to 0.017 when E11.5 $Sox10^{LacZ/+}$; $Zfhx1b^{\Delta/+}$ were compared to wild-type or $Zfhx1b^{\Delta/+}$ littermates). Careful analysis of TuJ1 staining at E11.5 allowed us to identify two types of TuJ1-positive cell population (see also (Stanchina et al., 2006)). One of these expresses a high level of TuJ1 and has long axonal processes (Fig. 6 E1); it is likely to correspond to post-mitotic neurons. The second population expresses a lower level of TuJ1, displays no axonal processes, and is likely to correspond to committed enteric neuroblasts (Fig. 6 E2). To quantify the two cell populations, we determined the percentage of "TuJ1-High" cells among the total population of neurons at E11.5. No significant difference in the relative proportion of these cells was observed between wild-type and single mutant embryos (Fig. 6 F). Indeed, the percentage of "TuJ1-High" among the total TuJ1 population in wild-type, $Zfhx1b^{\Delta/+}$, and $Sox10^{LacZ/+}$ cultures were $35 \pm 7\%$, $37 \pm 3\%$ and $48 \pm 10\%$ respectively (with p values ranging from $p = 0.74$ to 0.067). In contrast, we found a very significant increase in the relative proportion of "TuJ1-High" cells in double heterozygous mutants. Indeed, the percentage of "TuJ1-High" population reached $65 \pm 7\%$ in $Sox10^{LacZ/+}$;$Zfhx1b^{\Delta/+}$ (p ranging from 0.0005 to 0.031 when $Sox10^{LacZ/+}$;$Zfhx1b^{\Delta/+}$ embryos were compared to wild-type or $Sox10^{LacZ/+}$ littermates). Altogether, these results show that overall neuronal differentiation and/or terminal differentiation is increased in double heterozygous mutants. This increase could reduce the migration capacities of ENCC along the gut, and thus explains in part

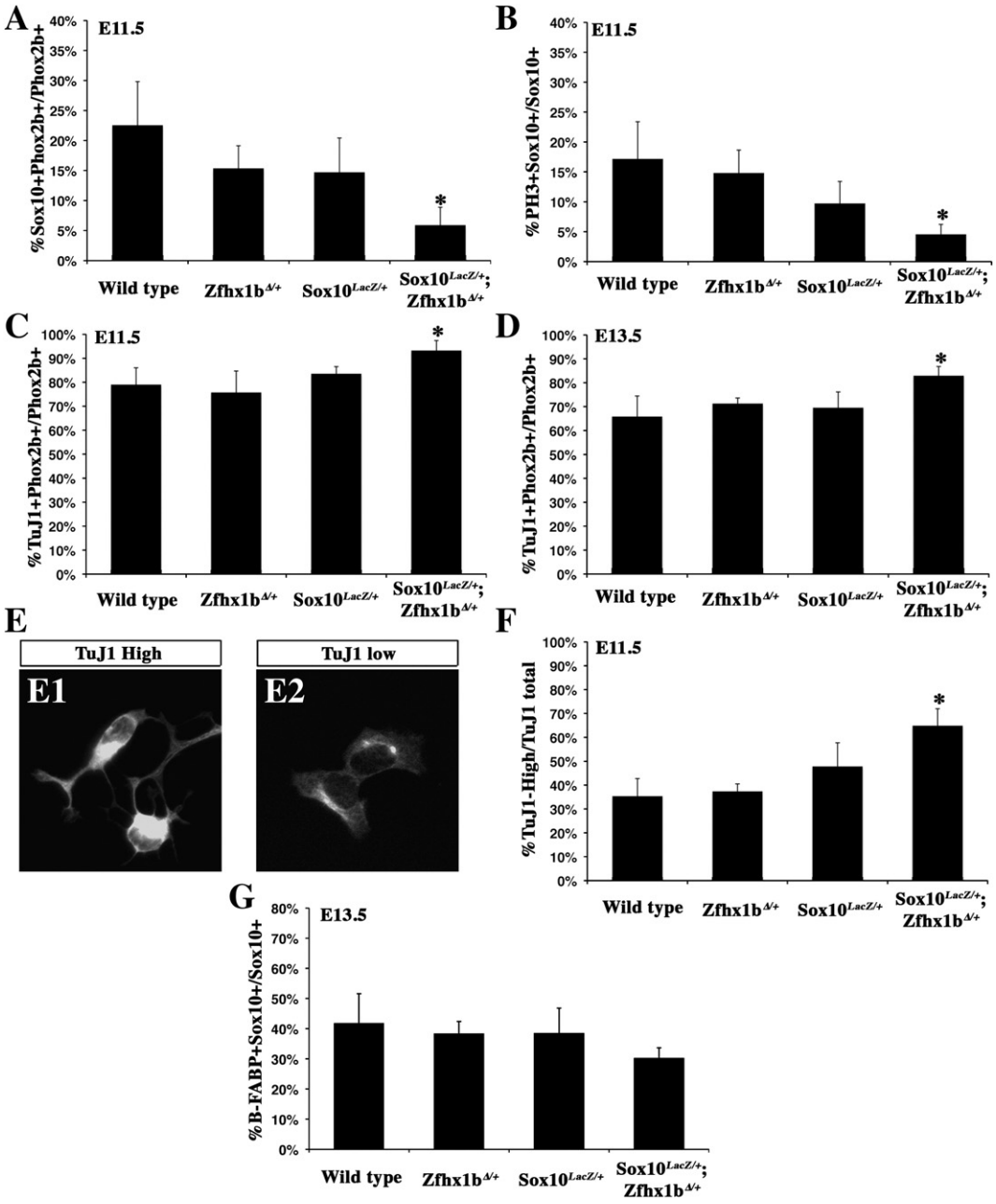

Fig. 6. Cellular origin of the ENS defects in E11.5 and E13.5 Sox10;Zfhx1b double mutants. (A) The pool of progenitor cells was quantified by counting the fraction of Phox2b positive cells co-labeled with Sox10 in acute dissociated gut cultures of E11.5 embryos of different genotypes. On average, 200 to 400 cells from 4 different embryos of each genotype were counted. Differences to the wild-type were statistically significant for Sox10$^{LacZ/+}$;Zfhx1b$^{\Delta/+}$ ($p=0.0058$). (B) Proliferation capacities of E11.5 enteric progenitor cells were quantified by counting the fraction of Sox10-positive cells co-labeled with phospho-histone 3. On average, 100 to 500 cells from 4 different embryos of each genotype were counted. Note the significant increased proliferation in Sox10$^{LacZ/+}$;Zfhx1b$^{\Delta/+}$ compared to controls ($p=0.006$). (C–D) Neuronal differentiation was quantified by counting the fraction of Phox2b positive cells co-labeled with TuJ1, reflecting the overall neuronal differentiation at E11.5 (C) and E13.5 (D). On average, 300 to 800 cells from 3 to 5 different embryos of each genotype were counted. Differences to the wild-type were statistically significant for Sox10$^{LacZ/+}$;Zfhx1b$^{\Delta/+}$ at both stages as determined by the Student's test ($p=0.0054$ and 0.04, respectively). (E) Careful examination of TuJ1 staining in E11.5 cultures revealed two types of TuJ1 cell population. One of these contains high levels of TuJ1 and has long axons ("TuJ1-High", E1). The second population expresses lower levels and has very few short axons ("TuJ1-Low", E2). (F) Quantification of "TuJ1-High" cells over the total population of TuJ1 positive cells in embryos of each genotype. Note the significant increased percentage of "TuJ1-High" cells in Sox10$^{LacZ/+}$;Zfhx1b$^{\Delta/+}$ compared to controls (wild-type, $p=0.0005$; and single mutants, $p<0.04$). (G) Quantification of the fraction of Sox10-positive cells co-labeled with the early B-FABP marker, reflecting glial differentiation at E13.5. On average, 200 cells from 5 different embryos of each genotype were counted. Differences with the wild-type embryo were not statistically significant ($p=0.184$).

the more severe ENS phenotype observed in double heterozygous mutants.

In parallel, we quantified the percentage of E13.5 ENCC specified to a glial fate by counting the percentage of Sox10-positive cells co-labeled with B-FABP. No significant change in the percentage of double-positive cells was observed in double heterozygous mutants compared to controls (Fig. 6 G), indicating that the deletion of one *Zfhx1b* allele in *Sox10* heterozygous mice does not affect glial cell differentiation.

Increased postnatal mortality of Sox10;Zfhx1b double mutants

In order to see if ENS defects observed in Sox10$^{LacZ/+}$;Zfhx1b$^{\Delta/+}$ embryos could be compensated beyond E13.5, we finally performed X-Gal staining on P5 guts from Sox10$^{LacZ/+}$;Zfhx1b$^{\Delta/+}$ and Sox10$^{LacZ/+}$ animals (Fig. 7). In parallel, we examined the postnatal survival of animals of different genotypes (Table 1). To this end, we intercrossed Sox10$^{LacZ/+}$ and Zfhx1b$^{\Delta/+}$ single mutants and analyzed, within the

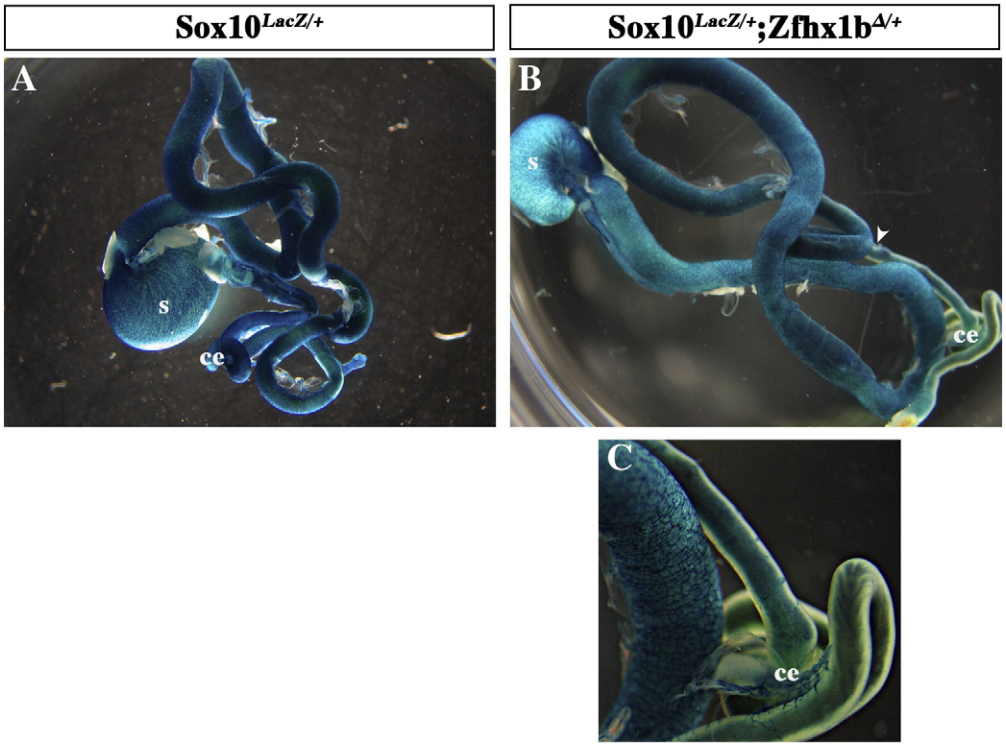

Fig. 7. Phenotypic analysis of newborn mice with combined Sox10 and Zfhx1b mutations. Whole-mount X-Gal staining of $Sox10^{LacZ/+}$ (A) and $Sox10^{LacZ/+}$;$Zfhx1b^{\Delta/+}$ (B) P5 guts. C represents a higher magnification of B showing ganglionic and aganglionic regions. s: stomach; ce: caecum. White arrowhead indicates the transition from stenotic to dilated gut segment.

progeny, the mortality of animals of each genotype up to 6 weeks after birth. At birth, all genotypes were represented in the expected Mendelian ratio. As previously reported, 92% of $Sox10^{LacZ/+}$ and all $Zfhx1b^{\Delta/+}$ survived up to 6 weeks of age and presented without enteric defects (Fig. 7 A and Table 1). In contrast, 70% of double heterozygous mice died within the first 4 weeks, and none survived after 6 weeks (Table 1). X-Gal staining at P5 confirmed the presence of ENS defects in all double mutants analyzed. The aganglionic segment often extended beyond the caecum and affected the first 1/3rd segment of the small intestine (2 animals analyzed, Fig. 7 B and C). As a consequence, faeces accumulated in front of the stenotic segment, distending the proximal innervated region (compare Fig. 7 A to B and C). Thus, removal of one *Zfhx1b* allele in *Sox10* heterozygous animals results in more severe ENS defects that are neither compensated during development nor after birth, and reduce the postnatal survival drastically.

Discussion

Zfhx1b is co-expressed with Sox10 during ENS development and Sox10; Zfhx1b double mutant mice studies reveal genetic interaction between both genes exclusively during ENS development

If the expression and function of SOX10 are well established, those of ZFHX1B remain elusive, and its interactions with other ENS genes are unknown. Here, we show that *Zfhx1b* is present with *Sox10* at all phases of ENS development. Both transcription factors are originally found in vagal neural crest cells migrating towards the gut, and in undifferentiated ENCC precursor cells. Later, their expression is maintained in GFAP-positive enteric glial cells, but is switched off during neuronal differentiation. Indeed, like SOX10, ZFHX1B is found in Mash1 positive cells (our unpublished results), but is absent in neuronal cells that contain TuJ1 or PGP9.5 markers ((Van de Putte et al., 2007) and this study). This profile contrasts sharply with the one described during brain cortex development. Indeed, a recent study showed that ZFHX1B protein is detected at the onset of cortical neurogenesis where high levels are found in post-mitotic neurons, but expression of this gene is barely detectable in progenitors (Miquelajauregui et al., 2007; Seuntjens et al., 2009). Whether these differences reflect diverse ZFHX1B functions and action mechanisms remain to be elucidated.

Based on the *Zfhx1b* and *Sox10* expression profiles, we speculated that both factors could be jointly required for proper ENS development. Through phenotype analysis of *Sox10;Zfhx1b* double mutants, we show that a coordinated and balanced interaction between these two genes is required for normal ENS development. Indeed, double mutants present with more severe ENS defects highlighting a strong genetic interaction between these two transcription factor-encoding genes.

Table 1
Genotypes distribution and viability analysis of animals resulting from $Sox10^{LacZ/+}$ and $Zfhx1b^{\Delta/+}$ crosses.

Genotypes	Number of animals genotyped	Number of animals dead between P0 and 4 weeks	Number of animals dead between 4 and 6 weeks	% of mortality over total period
$Sox10^{+/+}$;$Zfhx1b^{+/+}$	14	0	0	0%
$Sox10^{LacZ/+}$;$Zfhx1b^{+/+}$	13	1	0	8%
$Sox10^{+/+}$;$Zfhx1b^{\Delta/+}$	10	0	0	0%
$Sox10^{LacZ/+}$;$Zfhx1b^{\Delta/+}$	10	7	3	100%

Pup mortality was quantified by identifying all animals post mortem or at weaning (number of animals genotyped) and counting the number of animals dead between P0 and 4 weeks or P0 and 6 weeks.

We then documented the time point of earliest detectable ENS defects in double heterozygous mutant mice. With both genes already being co-expressed in vagal neural crest cells before/at the time ENCC enter the gut, we first tested interaction at E9.5 and E10.5. In contrast to Sox10;Sox8, Sox10;Edn3 and Sox10;Ednrb double mutants, we noticed an apparent normal ENS development in Sox10;Zfhx1b double heterozygous mutant embryos at these stages (Maka et al., 2005; Stanchina et al., 2006), suggesting that interaction between both factors only takes place when ENCC migrate along the gut.

To test this possibility, we analyzed the enteric phenotype of embryos of different genotypes from E11.5 up to P5. Using several markers, a dramatic reduction in the number of cells was seen in the intestine of $Sox10^{LacZ/+}$;$Zfhx1b^{\Delta/+}$ compared to single mutant littermates. The wavefront of migrating ENCC appeared severely delayed in all double heterozygous embryos and neonates that were analyzed. The affected segment always extended beyond the ileo-caecal junction, through the small intestine. We also examined the postnatal survival of the animals, and found that the mortality rate of 70%, four weeks after birth, in $Sox10^{LacZ/+}$;$Zfhx1b^{\Delta/+}$ clearly exceeds the 8% observed in $Sox10^{LacZ/+}$ animals on the same genetic background. Thus, the ablation of one *Zfhx1b* allele in *Sox10* heterozygous animals results in a more severe ENS phenotype from E11.5 onwards. These defects can never be compensated for. *Zfhx1b* therefore functions as a modifier gene for Sox10-dependent ENS defect as it increases both penetrance and severity of the defects in *Sox10* heterozygous mice despite having no detectable influence on ENS development on its own. Whether such a genetic interaction participates to the variability of Hirschsprung's disease phenotype observed among patients presenting with *SOX10* mutations remains to be clarified. However, these results highlight for the first time an interaction between two of the genes involved in syndromic forms of Hirschsprung disease, i.e. Mowat–Wilson syndrome and Waardenburg syndrome type 4.

Both factors are also present in other neural crest derivatives such as melanocytes, cranial ganglia, satellite glial cells and Schwann cells of the peripheral nervous system (Britsch et al., 2001; Van de Putte et al., 2007; Wegner, 2005). SOX10 and ZFHX1B are both present in melanoblasts, and their complete removal appears deleterious for melanocytes from the earlier stages of development (Van de Putte et al., 2007; Wegner, 2005). Moreover, *Sox10* and *Zfhx1b* null mouse embryos present with severe defects of DRG and Schwann cell development, highlighting an important function of both genes during glial cell development. Based on these observations, we have examined the formation and differentiation of these neural crest derivatives in E10.5 and E11.5 $Sox10^{LacZ/+}$;$Zfhx1b^{\Delta/+}$ embryos, but found no obvious extra defects, suggesting a specific cooperative requirement of both transcription factors in ENS development only.

Cellular origin of ENS defects observed in Sox10;Zfhx1b double heterozygous embryos

To decipher the cellular bases of the defects observed, we analyzed the proliferation, survival, and differentiation capacities of ENCC within the intestine of embryos of various genotypes. We observed a significant decrease (of about 50%) in the number of Sox10-positive progenitor cells in $Sox10^{LacZ/+}$;$Zfhx1b^{\Delta/+}$ embryos compared to controls. This reduction was not due to increased apoptosis, but rather is caused by a significant decrease (of about 50%) in their proliferation capacities. We believe that this reduction of enteric progenitor cells largely contributes to the more severe ENS phenotype observed in the double heterozygous mutants.

We also checked whether the combined deletion of *Sox10* and *Zfhx1b* affect neuronal and/or glial differentiation, which could explain the reduced migratory capacities of ENCC. We first analyzed overall neuronal differentiation, and observed a 15% increase in the number of neurons in double mutants. This slight but significant increase could contribute to the more severe ENS defects observed in $Sox10^{LacZ/+}$;$Zfhx1b^{\Delta/+}$ mutants. More importantly, careful examination of neuronal markers revealed that terminal differentiation maybe specifically accelerated. Indeed, we observed a 38% increase in the neuronal population presenting with "TuJ1-High" staining and long axonal processes in $Sox10^{LacZ/+}$;$Zfhx1b^{\Delta/+}$ compared to controls. Interestingly, these results resemble those described upon homozygous *Zfhx1b* deletion in the cortex. In the latter, the onset of neurogenesis is not altered upon *Zfhx1b* conditional deletion. However, once neurogenesis commences, the timing of production of different cell types is shifted to earlier stages (Seuntjens et al., 2009). This outcome is due to non-cell autonomous effects on progenitor cells, as ZFHX1B protein is not expressed in progenitor cells. In case of the ENS, we propose that the increase in neuronal differentiation could be due to a secondary effect that is visible only upon removal of one *Zfhx1b* allele in a *Sox10* heterozygote background. Alternatively, this increase in neuronal differentiation could be due to a combined action of SOX10 and ZFHX1B on neuronal differentiation, thus highlighting new cooperative functions of both factors during ENS development, but future experiments are required to test these possibilities.

In the brain cortex, the deletion of both *Zfhx1b* alleles also increased gliogenesis. The premature end of neurogenesis may pave the way for enhanced proliferation of glial precursors, which in turn leads to the production of a higher number of astrocytes (Seuntjens et al., 2009). We quantified the percentage of E13.5 ENCC specified to a glial fate, but partial removal of *Zfhx1b* in *Sox10* heterozygous does not seem to affect the ENS glial differentiation process at the stages observed.

Finally, partial loss of *Sox10* and *Zfhx1b* alleles could directly affect the migration of ENCC. A complete disorganization of the neuronal network was clearly visible in colonized regions of $Sox10^{LacZ/+}$;$Zfhx1b^{\Delta/+}$ embryos. In line with these observations, it is important to mention that BMPs control many aspects of ENS development, including differentiation, proliferation, and survival of ENCC (Chalazonitis et al., 2004, 2008; De Santa Barbara et al., 2005). In addition, activation of BMPs signaling reduces the rate of ENCC migration, encourages ganglion cell aggregation, enhances neurite fasciculation, controls radial migration within the bowel wall, and influences the orientation of nerve fibers within plexuses (Fu et al., 2006; Goldstein et al., 2005). The clustering of ENCC and alteration of the pattern of neurite extension observed upon treatment with BMP2 and BMP4 are very similar to the network disorganization observed in this study (Fu et al., 2006). Combined reduction of *Sox10* and *Zfhx1b* levels could therefore increase BMP activity (see below), and thus alter cell migration/adhesion and neurite extension. This, of course does not rule out that both factors have additional consecutive roles in ENS development, which might be less sensitive to dosage effects.

Of note, ZFHX1B was also found in non-crest derived cells during ENS development, i.e. in mesenchymal cells adjacent to the epithelium ((Van de Putte et al., 2007) and this study), in a region previously described as containing BMPs-expressing cells (Fu et al., 2006). Interestingly, modulation of mesodermal BMP signaling pathway in the hindgut affected all tissues layers: mesenchyme–smooth muscle, ENS and endoderm–epithelium (De Santa Barbara et al., 2005). This suggests that ZFHX1B could control ENS development in both a cell autonomous and non-cell autonomous manner. We therefore cannot exclude the possibility that this mesenchymal Zfhx1b expression could be partly responsible for the phenotype observed in double mutants.

Molecular origin of ENS defects observed in double heterozygous mutant mice and implication for ENS formation

The *Sox10*/*Zfhx1b* interaction we detected here could be explained by different molecular mechanisms. SOX10 could regulate *Zfhx1b*

transcription or vice versa; both of them could also act on independent target genes that activate a common cascade; or act as co-factors regulating the expression of common target genes in a synergistic manner. Finally, both could be part of a common signaling pathway, linked by indirect mechanisms. In order to gain insight into these possibilities, we first decided to analyze the effect of ZFHX1B on *Sox10* expression and vice versa. Several *Sox10* enhancers were recently described (Antonellis et al., 2006, 2008; Deal et al., 2006; Dutton et al., 2008; Werner et al., 2007). Two of them seem essential to drive *Sox10* expression in ENS (Antonellis et al., 2008; Werner et al., 2007). Interestingly, both sequences contain putative ZFHX1B binding sites. Integrative genomic analysis of *ZFHX1B* was also very recently carried out but no SOX binding sites were reported in the analyzed regions (Katoh, 2009). Based on these observations, we used luciferase assays and RT-PCR experiments to test i) the effect of ZFHX1B on the two SOX10 regulatory sequences of interest and ii) the effect of SOX10 overexpression on *Zfhx1b* expression, without success.

We cannot exclude that both transcription factors could act as co-factors regulating the expression of common target genes in a synergistic manner, but SOX proteins have to our knowledge not been identified in the ZFHX1B proteome or picked-up in protein–protein interactions screenings. With the data presently available, we propose an indirect link, via modulation of *Bmp* gene expression as the molecular origin of the ENS defects observed. Kim et al. reported that SOX10 preserves not only glial but – surprisingly – also neuronal differentiation potential. The latter function is reflected in the requirement of SOX10 *in vivo* and *in vitro* for induction of Mash1 and Phox2b. Simultaneously, SOX10 inhibits or delays neuronal differentiation by repressing Phox2a. However, this activity requires higher *Sox10* gene dosage (Kim et al., 2003). In addition, application of BMP ligand to NCC cultures caused SOX10 extinction within 24 hours. Whether this action is direct or indirect, affects gene or protein levels is not known, but these results clearly show that downregulation of SOX10 is an early event in the rapid lineage restriction promoted by BMP signaling (Kim et al., 2003). Independently, experiments performed in *Xenopus* have shown that XSIP1 (ZFHX1B) is required for inhibition of BMP signaling (van Grunsven et al., 2007): ZFHX1B binds directly to the *bmp4* promoter and represses its activity. If all these regulations also take place during ENS development, we can speculate that a reduction of ZFHX1B could lead to increased BMP activity, which in turn could cause downregulation of SOX10. In the context of *Sox10* heterozygous animals, this extra reduction could be critical and lead to increased *Phox2a* transcription (or of other neuronal markers) and accelerated neuronal differentiation, thus explaining part of the cellular defects observed in double mutants. Although further work will be necessary to fully understand ZFHX1B function during ENS throughout development and the molecular origin of the ENS defects observed upon combined deletion of the *Sox10* and *Zfhx1b* alleles, the data presented here suggest that these two transcription factors could work together to control ENS stem cell maintenance and neuronal differentiation. Whether Zfhx1b interacts with other ENS genes known to control ENS progenitor maintenance remains to be tested. Interestingly, Seuntjens et al. suggested that ZFHX1B could restrain the production of signaling factors produced in post-mitotic neurons that feed back to progenitor cells to regulate the timing of cell fate switch and the number of neurons and glial cells (Seuntjens et al., 2009). In line with these observations, it would be very interesting to test the possibility that ZFHX1B could control – or be under the control of – signaling factors such as GDNF, or endothelin-3, and thus control the pool size of ENCC and their differentiation.

Taken altogether, our results contribute to improve our understanding of the cellular and genetic bases of the enteric defects observed in mice and humans affected by *SOX10* and *ZFHX1B* mutations. They definitely further extend the molecular network that governs proper ENS development.

Acknowledgments

We thank Mohamed Bouaziz for animal husbandry and Natacha Martin for animal genotyping. This work was supported by INSERM and Agence Nationale de la Recherche grant ANR-05-MRAR-008-01. LS was supported by a research fellowship from the Fondation pour la Recherche Médicale (FRM). Research in the DH lab was supported by FWO-Flanders (project G.0288.07), the Inter-Universitary Attraction Pole Network (IUAP-PAI 6/20) and the EC FP6 Integrated Project Endotrack (LSHG-CT-2006-19050).

References

Amiel, J., Sproat-Emison, E., Garcia-Barcelo, M., Lantieri, F., Burzynski, G., Borrego, S., Pelet, A., Arnold, S., Miao, X., Griseri, P., Brooks, A.S., Antinolo, G., de Pontual, L., Clement-Ziza, M., Munnich, A., Kashuk, C., West, K., Wong, K.K., Lyonnet, S., Chakravarti, A., Tam, P.K., Ceccherini, I., Hofstra, R.M., Fernandez, R., 2008. Hirschsprung disease, associated syndromes and genetics: a review. J. Med. Genet. 45, 1–14.

Antonellis, A., Bennett, W.R., Menheniott, T.R., Prasad, A.B., Lee-Lin, S.Q., Green, E.D., Paisley, D., Kelsh, R.N., Pavan, W.J., Ward, A., 2006. Deletion of long-range sequences at Sox10 compromises developmental expression in a mouse model of Waardenburg-Shah (WS4) syndrome. Hum. Mol. Genet. 15, 259–271.

Antonellis, A., Huynh, J.L., Lee-Lin, S.Q., Vinton, R.M., Renaud, G., Loftus, S.K., Elliot, G., Wolfsberg, T.G., Green, E.D., McCallion, A.S., Pavan, W.J., 2008. Identification of neural crest and glial enhancers at the mouse Sox10 locus through transgenesis in zebrafish. PLoS Genet. 4, e1000174.

Barlow, A., de Graaff, E., Pachnis, V., 2003. Enteric nervous system progenitors are coordinately controlled by the G protein-coupled receptor EDNRB and the receptor tyrosine kinase RET. Neuron. 40, 905–916.

Bassez, G., Camand, O.J., Cacheux, V., Kobetz, A., Dastot-Le Moal, F., Marchant, D., Catala, M., Abitbol, M., Goossens, M., 2004. Pleiotropic and diverse expression of ZFHX1B gene transcripts during mouse and human development supports the various clinical manifestations of the "Mowat–Wilson" syndrome. Neurobiol. Dis. 15, 240–250.

Bondurand, N., Natarajan, D., Barlow, A., Thapar, N., Pachnis, V., 2006. Maintenance of mammalian enteric nervous system progenitors by SOX10 and endothelin 3 signalling. Development 133, 2075–2086.

Bondurand, N., Natarajan, D., Thapar, N., Atkins, C., Pachnis, V., 2003. Neuron and glia generating progenitors of the mammalian enteric nervous system isolated from foetal and postnatal gut cultures. Development 130, 6387–6400.

Bowles, J., Schepers, G., Koopman, P., 2000. Phylogeny of the SOX family of developmental transcription factors based on sequence and structural indicators. Dev. Biol. 227, 239–255.

Britsch, S., Goerich, D.E., Riethmacher, D., Peirano, R.I., Rossner, M., Nave, K.A., Birchmeier, C., Wegner, M., 2001. The transcription factor Sox10 is a key regulator of peripheral glial development. Genes Dev. 15, 66–78.

Burns, A.J., Douarin, N.M., 1998. The sacral neural crest contributes neurons and glia to the post-umbilical gut: spatiotemporal analysis of the development of the enteric nervous system. Development 125, 4335–4347.

Burns, A.J., Thapar, N., 2006. Advances in ontogeny of the enteric nervous system. Neurogastroenterol. Motil. 18, 876–887.

Burzynski, G., Shepherd, I.T., Enomoto, H., 2009. Genetic model system studies of the development of the enteric nervous system, gut motility and Hirschsprung's disease. Neurogastroenterol. Motil. 21, 113–127.

Cacheux, V., Dastot-Le Moal, F., Kaariainen, H., Bondurand, N., Rintala, R., Boissier, B., Wilson, M., Mowat, D., Goossens, M., 2001. Loss-of-function mutations in SIP1 Smad interacting protein 1 result in a syndromic Hirschsprung disease. Hum. Mol. Genet. 10, 1503–1510.

Cantrell, V.A., Owens, S.E., Chandler, R.L., Airey, D.C., Bradley, K.M., Smith, J.R., Southard-Smith, E.M., 2004. Interactions between Sox10 and EdnrB modulate penetrance and severity of aganglionosis in the Sox10Dom mouse model of Hirschsprung disease. Hum. Mol. Genet. 13, 2289–2301.

Chalazonitis, A., D'Autreaux, F., Guha, U., Pham, T.D., Faure, C., Chen, J.J., Roman, D., Kan, L., Rothman, T.P., Kessler, J.A., Gershon, M.D., 2004. Bone morphogenetic protein-2 and -4 limit the number of enteric neurons but promote development of a TrkC-expressing neurotrophin-3-dependent subset. J. Neurosci. 24, 4266–4282.

Chalazonitis, A., Pham, T.D., Li, Z., Roman, D., Guha, U., Gomes, W., Kan, L., Kessler, J.A., Gershon, M.D., 2008. Bone morphogenetic protein regulation of enteric neuronal phenotypic diversity: relationship to timing of cell cycle exit. J. Comp. Neurol. 509, 474–492.

Comijn, J., Berx, G., Vermassen, P., Verschueren, K., van Grunsven, L., Bruyneel, E., Mareel, M., Huylebroeck, D., van Roy, F., 2001. The two-handed E box binding zinc finger protein SIP1 downregulates E-cadherin and induces invasion. Mol. Cell 7, 1267–1278.

Dastot-Le Moal, F., Wilson, M., Mowat, D., Collot, N., Niel, F., Goossens, M., 2007. ZFHX1B mutations in patients with Mowat–Wilson syndrome. Hum. Mutat. 28, 313–321.

De Santa Barbara, P., Williams, J., Goldstein, A.M., Doyle, A.M., Nielsen, C., Winfield, S., Faure, S., Roberts, D.J., 2005. Bone morphogenetic protein signaling pathway plays multiple roles during gastrointestinal tract development. Dev. Dyn. 234, 312–322.

Deal, K.K., Cantrell, V.A., Chandler, R.L., Saunders, T.L., Mortlock, D.P., Southard-Smith, E. M., 2006. Distant regulatory elements in a Sox10-beta GEO BAC transgene are

required for expression of Sox10 in the enteric nervous system and other neural crest-derived tissues. Dev. Dyn. 235, 1413–1432.
Delalande, J.M., Guyote, M.E., Smith, C.M., Shepherd, I.T., 2008. Zebrafish sip1a and sip1b are essential for normal axial and neural patterning. Dev. Dyn. 237, 1060–1069.
Dutton, J.R., Antonellis, A., Carney, T.J., Rodrigues, F.S., Pavan, W.J., Ward, A., Kelsh, R.N., 2008. An evolutionarily conserved intronic region controls the spatiotemporal expression of the transcription factor Sox10. BMC Dev. Biol. 8, 105.
Eisaki, A., Kuroda, H., Fukui, A., Asashima, M., 2000. XSIP1, a member of two-handed zinc finger proteins, induced anterior neural markers in Xenopus laevis animal cap. Biochem. Biophys. Res. Commun. 271, 151–157.
Espinosa-Parrilla, Y., Amiel, J., Auge, J., Encha-Razavi, F., Munnich, A., Lyonnet, S., Vekemans, M., Attie-Bitach, T., 2002. Expression of the SMADIP1 gene during early human development. Mech. Dev. 114, 187–191.
Fu, M., Vohra, B.P., Wind, D., Heuckeroth, R.O., 2006. BMP signaling regulates murine enteric nervous system precursor migration, neurite fasciculation, and patterning via altered Ncam1 polysialic acid addition. Dev. Biol. 299, 137–150.
Furness, J., 2006. The enteric nervous system.
Garavelli, L., Zollino, M., Mainardi, P.C., Gurrieri, F., Rivieri, F., Soli, F., Verri, R., Albertini, E., Favaron, E., Zignani, M., Orteschi, D., Bianchi, P., Faravelli, F., Forzano, F., Seri, M., Wischmeijer, A., Turchetti, D., Pompilii, E., Gnoli, M., Cocchi, G., Mazzanti, L., Bergamaschi, R., De Brasi, D., Sperandeo, M.P., Mari, F., Uliana, V., Mostardini, R., Cecconi, M., Grasso, M., Sassi, S., Sebastio, G., Renieri, A., Silengo, M., Bernasconi, S., Wakamatsu, N., Neri, G., 2009. Mowat–Wilson syndrome: facial phenotype changing with age: study of 19 Italian patients and review of the literature. Am. J. Med. Genet. 149A, 417–426.
Gershon, M.D.K., A.L., Wade, P.R., 1994. Functional Anatomy of the Enteric Nervous System. Raven Press, New York.
Goldstein, A.M., Brewer, K.C., Doyle, A.M., Nagy, N., Roberts, D.J., 2005. BMP signaling is necessary for neural crest cell migration and ganglion formation in the enteric nervous system. Mech. Dev. 122, 821–833.
Hao, M.M., Young, H.M., 2009. Development of enteric neuron diversity. J. Cell Mol. Med.
Heanue, T.A., Pachnis, V., 2007. Enteric nervous system development and Hirschsprung's disease: advances in genetic and stem cell studies. Nat. Rev. Neurosci. 8, 466–479.
Herbarth, B., Pingault, V., Bondurand, N., Kuhlbrodt, K., Hermans-Borgmeyer, I., Puliti, A., Lemort, N., Goossens, M., Wegner, M., 1998. Mutation of the Sry-related Sox10 gene in Dominant megacolon, a mouse model for human Hirschsprung disease. Proc. Natl. Acad. Sci. U. S. A. 95, 5161–5165.
Higashi, Y., Maruhashi, M., Nelles, L., Van de Putte, T., Verschueren, K., Miyoshi, T., Yoshimoto, A., Kondoh, H., Huylebroeck, D., 2002. Generation of the floxed allele of the SIP1 (Smad-interacting protein 1) gene for Cre-mediated conditional knockout in the mouse. Genesis 32, 82–84.
Honore, S.M., Aybar, M.J., Mayor, R., 2003. Sox10 is required for the early development of the prospective neural crest in Xenopus embryos. Dev. Biol. 260, 79–96.
Kapur, R.P., 1999. Early death of neural crest cells is responsible for total enteric aganglionosis in Sox10(Dom)/Sox10(Dom) mouse embryos. Pediatr. Dev. Pathol. 2, 559–569.
Katoh, M., 2009. Integrative genomic analyses of ZEB2: transcriptional regulation of ZEB2 based on SMADs, ETS1, HIF1alpha, POU/OCT, and NF-kappaB. Int. J. Oncol. 34, 1737–1742.
Kelsh, R.N., 2006. Sorting out Sox10 functions in neural crest development. Bioessays 28, 788–798.
Kim, J., Lo, L., Dormand, E., Anderson, D.J., 2003. SOX10 maintains multipotency and inhibits neuronal differentiation of neural crest stem cells. Neuron 38, 17–31.
Kurtz, A., Zimmer, A., Schnutgen, F., Bruning, G., Spener, F., Muller, T., 1994. The expression pattern of a novel gene encoding brain-fatty acid binding protein correlates with neuronal and glial cell development. Development 120, 2637–2649.
Lang, D., Chen, F., Milewski, R., Li, J., Lu, M.M., Epstein, J.A., 2000. Pax3 is required for enteric ganglia formation and functions with Sox10 to modulate expression of c-ret. J. Clin. Invest. 106, 963–971.
Le Douarin, N.M., Kalcheim, C., 1999. The Neural Crest. Cambridge University Press, Cambridge.
Maka, M., Stolt, C.C., Wegner, M., 2005. Identification of Sox8 as a modifier gene in a mouse model of Hirschsprung disease reveals underlying molecular defect. Dev. Biol. 277, 155–169.
Miquelajauregui, A., Van de Putte, T., Polyakov, A., Nityanandam, A., Boppana, S., Seuntjens, E., Karabinos, A., Higashi, Y., Huylebroeck, D., Tarabykin, V., 2007. Smad-interacting protein-1 (Zfhx1b) acts upstream of Wnt signaling in the mouse hippocampus and controls its formation. Proc. Natl. Acad. Sci. U. S. A. 104, 12919–12924.
Mollaaghababa, R., Pavan, W.J., 2003. The importance of having your SOX on: role of SOX10 in the development of neural crest-derived melanocytes and glia. Oncogene 22, 3024–3034.
Nitta, K.R., Takahashi, S., Haramoto, Y., Fukuda, M., Tanegashima, K., Onuma, Y., Asashima, M., 2007. The N-terminus zinc finger domain of Xenopus SIP1 is important for neural induction, but not for suppression of Xbra expression. Int. J. Dev. Biol. 51, 321–325.
Nitta, K.R., Tanegashima, K., Takahashi, S., Asashima, M., 2004. XSIP1 is essential for early neural gene expression and neural differentiation by suppression of BMP signaling. Dev. Biol. 275, 258–267.
Owens, S.E., Broman, K.W., Wiltshire, T., Elmore, J.B., Bradley, K.M., Smith, J.R., Southard-Smith, E.M., 2005. Genome-wide linkage identifies novel modifier loci of aganglionosis in the Sox10Dom model of Hirschsprung disease. Hum. Mol. Genet. 14, 1549–1558.
Paratore, C., Eichenberger, C., Suter, U., Sommer, L., 2002. Sox10 haploinsufficiency affects maintenance of progenitor cells in a mouse model of Hirschsprung disease. Hum. Mol. Genet. 11, 3075–3085.
Pattyn, A., Morin, X., Cremer, H., Goridis, C., Brunet, J.F., 1997. Expression and interactions of the two closely related homeobox genes Phox2a and Phox2b during neurogenesis. Development 124, 4065–4075.
Postigo, A.A., 2003. Opposing functions of ZEB proteins in the regulation of the TGFbeta/BMP signaling pathway. EMBO J. 22, 2443–2452.
Postigo, A.A., Dean, D.C., 2000. Differential expression and function of members of the zfh-1 family of zinc finger/homeodomain repressors. Proc. Natl. Acad. Sci. U. S. A. 97, 6391–6396.
Seuntjens, E., Nityanandam, A., Miquelajauregui, A., Debruyn, J., Stryjewska, A., Goebbels, S., Nave, K.A., Huylebroeck, D., Tarabykin, V., 2009. Sip1 regulates sequential fate decisions by feedback signaling from postmitotic neurons to progenitors. Nat. Neurosci.
Southard-Smith, E.M., Kos, L., Pavan, W.J., 1998. Sox10 mutation disrupts neural crest development in Dom Hirschsprung mouse model. Nat. Genet. 18, 60–64.
Stanchina, L., Baral, V., Robert, F., Pingault, V., Lemort, N., Pachnis, V., Goossens, M., Bondurand, N., 2006. Interactions between Sox10, Edn3 and Ednrb during enteric nervous system and melanocyte development. Dev. Biol. 295, 232–249.
Van de Putte, T., Francis, A., Nelles, L., van Grunsven, L.A., Huylebroeck, D., 2007. Neural crest-specific removal of Zfhx1b in mouse leads to a wide range of neurocristopathies reminiscent of Mowat—Wilson syndrome. Hum. Mol. Genet. 16, 1423–1436.
Van de Putte, T., Maruhashi, M., Francis, A., Nelles, L., Kondoh, H., Huylebroeck, D., Higashi, Y., 2003. Mice lacking ZFHX1B, the gene that codes for Smad-interacting protein-1, reveal a role for multiple neural crest cell defects in the etiology of Hirschsprung disease–mental retardation syndrome. Am. J. Hum. Genet. 72, 465–470.
van Grunsven, L.A., Michiels, C., Van de Putte, T., Nelles, L., Wuytens, G., Verschueren, K., Huylebroeck, D., 2003. Interaction between Smad-interacting protein-1 and the corepressor C-terminal binding protein is dispensable for transcriptional repression of E-cadherin. J. Biol. Chem. 278, 26135–26145.
van Grunsven, L.A., Schellens, A., Huylebroeck, D., Verschueren, K., 2001. SIP1 (Smad interacting protein 1) and deltaEF1 (delta-crystallin enhancer binding factor) are structurally similar transcriptional repressors. J. Bone Joint Surg. Am. 83-A (Suppl 1), S40–S47.
van Grunsven, L.A., Taelman, V., Michiels, C., Verstappen, G., Souopgui, J., Nichane, M., Moens, E., Opdecamp, K., Vanhomwegen, J., Kricha, S., Huylebroeck, D., Bellefroid, E.J., 2007. XSip1 neuralizing activity involves the co-repressor CtBP and occurs through BMP dependent and independent mechanisms. Dev. Biol. 306, 34–49.
Vandewalle, C., Comijn, J., De Craene, B., Vermassen, P., Bruyneel, E., Andersen, H., Tulchinsky, E., Van Roy, F., Berx, G., 2005. SIP1/ZEB2 induces EMT by repressing genes of different epithelial cell–cell junctions. Nucleic Acids Res. 33, 6566–6578.
Verschueren, K., Remacle, J.E., Collart, C., Kraft, H., Baker, B.S., Tylzanowski, P., Nelles, L., Wuytens, G., Su, M.T., Bodmer, R., Smith, J.C., Huylebroeck, D., 1999. SIP1, a novel zinc finger/homeodomain repressor, interacts with Smad proteins and binds to 5′-CACCT sequences in candidate target genes. J. Biol. Chem. 274, 20489–20498.
Wakamatsu, N., Yamada, Y., Yamada, K., Ono, T., Nomura, N., Taniguchi, H., Kitoh, H., Mutoh, N., Yamanaka, T., Mushiake, K., Kato, K., Sonta, S., Nagaya, M., 2001. Mutations in SIP1, encoding Smad interacting protein-1, cause a form of Hirschsprung disease. Nat. Genet. 27, 369–370.
Wegner, M., 1999. From head to toes: the multiple facets of Sox proteins. Nucleic Acids Res. 27, 1409–1420.
Wegner, M., 2005. Secrets to a healthy Sox life: lessons for melanocytes. Pigment Cell Res. 18, 74–85.
Wegner, M., 2009. All purpose Sox: the many roles of Sox proteins in gene expression. Int. J. Biochem. Cell Biol.
Werner, T., Hammer, A., Wahlbuhl, M., Bosl, M.R., Wegner, M., 2007. Multiple conserved regulatory elements with overlapping functions determine Sox10 expression in mouse embryogenesis. Nucleic Acids Res. 35, 6526–6538.
Wilson, M., Koopman, P., 2002. Matching SOX: partner proteins and co-factors of the SOX family of transcriptional regulators. Curr. Opin. Genet. Dev. 12, 441–446.
Young, H.M., Bergner, A.J., Muller, T., 2003. Acquisition of neuronal and glial markers by neural crest-derived cells in the mouse intestine. J. Comp. Neurol. 456, 1–11.
Zhu, L., Lee, H.O., Jordan, C.S., Cantrell, V.A., Southard-Smith, E.M., Shin, M.K., 2004. Spatiotemporal regulation of endothelin receptor-B by SOX10 in neural crest-derived enteric neuron precursors. Nat. Genet. 36, 732–737.
Zweier, C., Thiel, C.T., Dufke, A., Crow, Y.J., Meinecke, P., Suri, M., Ala-Mello, S., Beemer, F., Bernasconi, S., Bianchi, P., Bier, A., Devriendt, K., Dimitrov, B., Firth, H., Gallagher, R.C., Garavelli, L., Gillessen-Kaesbach, G., Hudgins, L., Kaariainen, H., Karstens, S., Krantz, I., Mannhardt, A., Medne, L., Mucke, J., Kibaek, M., Krogh, L.N., Peippo, M., Rittinger, O., Schulz, S., Schelley, S.L., Temple, I.K., Dennis, N.R., Van der Knaap, M.S., Wheeler, P., Yerushalmi, B., Zenker, M., Seidel, H., Lachmeijer, A., Prescott, T., Kraus, C., Lowry, R.B., Rauch, A., 2005. Clinical and mutational spectrum of Mowat–Wilson syndrome. Eur. J. Med. Genet. 48, 97–111.